Growth of *Escherichia coli* on the GaAs (001) surface

Elnaz Nazemi, Walid M. Hassen, Eric H. Frost, Jan J. Dubowski

www.elsevier.com/locate/talanta

PII: S0039-9140(17)30906-2
DOI: http://dx.doi.org/10.1016/j.talanta.2017.08.097
Reference: TAL17893

To appear in: *Talanta*

Received date: 6 June 2017
Revised date: 23 August 2017
Accepted date: 24 August 2017

Cite this article as: Elnaz Nazemi, Walid M. Hassen, Eric H. Frost and Jan J. Dubowski, Growth of *Escherichia coli* on the GaAs (001) surface, *Talanta,* http://dx.doi.org/10.1016/j.talanta.2017.08.097

Growth of *Escherichia coli* on the GaAs (001) surface

Elnaz Nazemi[a], Walid M. Hassen[a], Eric H. Frost[a,b] and Jan J. Dubowski[a*]

[a] Interdisciplinary Institute for Technological Innovation (3IT), CNRS UMI-3463, Department of Electrical and Computer Engineering, Faculty of Engineering, Université de Sherbrooke, 3000, boul. de l'Université, Sherbrooke, Québec J1K 0A5, Canada

[b] Department of Microbiology and Infectiology, Faculty of Medicine and Health Sciences, Université de Sherbrooke, 3001, 12th Avenue North, Sherbrooke, Québec J1H 5N4, Canada

Email of authors: Elnaz Nazemi (Elnaz.Nazemi@usherbrooke.ca); Walid M. Hassen (mohamed.walid.hassen@usherbrooke.ca); Eric H. Frost (Eric.Frost@usherbrooke.ca); Jan J. Dubowski (Jan.J.Dubowski@usherbrooke.ca)

[*]Correspondence: Jan.J.Dubowski@usherbrooke.ca

Interdisciplinary Institute for Technological Innovation (3IT), Laboratory for Quantum Semiconductors and Photon-based BioNanotechnology, Université de Sherbrooke, 3000, boul. de l'Université, Sherbrooke, Québec J1K 0A5, Canada

Abbreviations

CFU**,** Colony forming unit; PCR, Polymerase chain reaction; SPR, Surface plasmon resonance; PL, Photoluminescence; SI, Semi-insulating; DI water, Deionized water; AS, Ammonium sulfide; b-PEG, Biotinylated polyethylene glycol; LB, Luria Bertani; PBS, Phosphate buffered saline; MHDA, 16-Mercaptohexadecanoic acid; HDT, Hexadecanethiol; EDC, 1-Ethyl-3-(3-dimethylaminopropyl)-carbodiimide; NHS, N-hydroxysuccinimide; Ab, Non-conjugated polyclonal antibodies; b-Ab, Polyclonal biotinylated antibodies; NA, Neutravidin; SAM, Self-assembled monolayer; FTIR, Fourier transform infrared spectroscopy

Abstract

Detection of pathogenic bacteria and monitoring their susceptibility to antibiotics are of great importance in the fields of medicine, pharmaceutical research, as well as water and food industries. In order to develop a photonic biosensor for detection of bacteria by taking advantage of photoluminescence (PL) of GaAs-based devices, we have investigated the capture and growth of *Escherichia coli* K12 on bare and biofunctionalized surfaces of GaAs (001) - a material of interest for capping different semiconductor microstructures. The results were compared with the capture and growth of *Escherichia coli* K12 on Au surfaces that have commonly been applied for studying a variety of biological and biochemical reactions. We found that neither GaAs nor Au-coated glass wafers placed in Petri dishes with nutrient agar inoculated bacteria inhibited bacterial growth, regardless of the wafers being bare or biofunctionalized. However, the capture and growth of bacteria on biofunctionalized surfaces of GaAs and Au wafers kept in a flow cell and exposed to different concentrations of bacteria and growth medium revealed that the initial surface coverage and the subsequent bacterial growth were dependent on the biofunctionalization architecture, with antibody-coated surfaces clearly being most efficient in capturing bacteria and offering better conditions for growth of bacteria. We have observed that, as long as the GaAs wafers were exposed to bacterial suspensions at concentrations of at least 10^5 CFU/mL, bacteria could grow on the surface of wafers, regardless of the type of biofunctionalization architecture used to capture the bacteria. These results provide important insight towards the successful development of GaAs-based devices designed for photonic monitoring of bacterial reactions to different biochemical environments.

Graphical abstract

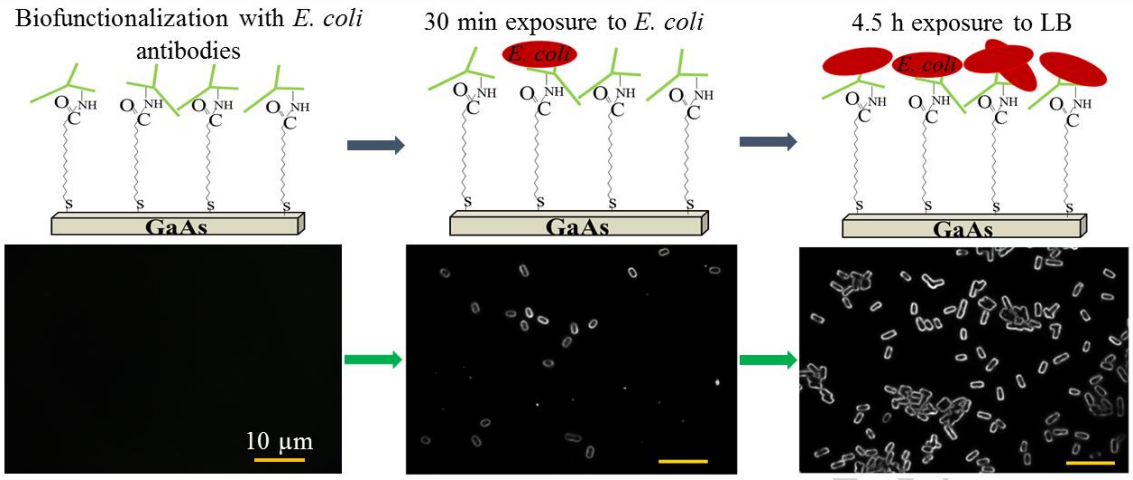

Keywords: GaAs-based biosensor, Photocorrosion, Self-assembled monolayer, Antibody, *Escherichia coli*, Bacterial growth,

Introduction

Evaluating growth of bacteria to determine antibiotic susceptibility and metabolic traits is essential to diagnostic microbiology [1]. Monitoring the viability, growth and cellular metabolism of bacteria also plays an important role in yielding bacterial products in industrial- or small-scale experiments [2-6]. Conventionally, bacterial growth has been investigated by (1) plate counting where colony forming units (CFU) are determined [2], and (2) visualization of growth in broth either by eye or by nephelometry [1, 7, 8]. Broth microdilution and Kirby-Bauer disk diffusion are widely applied in clinical laboratories to evaluate the antibiotic susceptibility of bacteria [1, 9]. These techniques are time-consuming and labour intensive and, typically, they are not able to provide same-day monitoring [1, 6, 10]. Polymerase chain reaction (PCR) [1, 11, 12], surface plasmon resonance (SPR) [10] and fluorescence-based assays [13, 14] have been introduced for rapid evaluation of growth and antimicrobial sensitivity of bacteria. However, the cost of PCR [15] and SPR systems [16] and technical complexity of using fluorescent dyes are inhibitory factors that limit the application of these methods in clinical laboratories.

Photoluminescence (PL) emitting semiconductors hold a great potential for biosensing applications due to the sensitivity of the PL signal to the surface localized phenomena [17-21]. Electrically charged molecules, if immobilized at the surface of such semiconductors, could affect their PL by modifying bending of their energy bands near the surface [22, 23]. PL of some semiconductors has been used for chemical sensing [22] and detection of biomolecules [24]. We have demonstrated a successful detection of electrically charged viruses [25], *Escherichia coli* K12 bacteria [26, 27] and, more recently, *Legionella pneumophila* [28] by taking advantage of PL emission of

GaAs/AlGaAs (001) nano-heterostructures. The major advantage of the GaAs/AlGaAs based biosensors, in comparison to a variety of biosensors employing Au surfaces, is their low cost. Note that GaAs (001) denotes a specific, technologically important surface of a zinc blende crystal structure GaAs material [29, 30] that is well-known in the production of optoelectronic devices [31, 32]. While a ubiquitous presence of GaAs/AlGaAs microstructures in light emitting diodes and other commercial devices suggests that they should be relatively inexpensive, an additional attractive feature of the GaAs/AlGaAs based biosensor is the inexpensive hardware required for reading the biosensor PL signal. We have recently demonstrated that PL emission of GaAs/AlGaAs microstructures could be employed to monitor the growth and antibiotic susceptibility of *Escherichia coli* immobilized on the surface of such microstructures [33]. One of the key elements in the development of this innovative biosensing platform is to investigate the mechanisms of interaction between bacteria and the GaAs (001) compound used for capping PL emitting GaAs/AlGaAs microstructures, as well as to determine conditions for the optimized immobilization and growth of bacteria.

Growth of bacteria on solid surfaces can be affected by biocompatibility of the substrate. Some metal surfaces such as silver (Ag) are well-known to have antimicrobial activity and prevent bacterial colonization [34]. Silver coating is widely applied for reducing bacterial contamination of medical tools and minimizing nosocomial infections related to operating rooms and other sections of hospitals [35]. Some gold (Au)-coated nanoparticles were found toxic to bacteria [36], whereas others were not [37]. Furthermore, arsenic (As) and gallium (Ga) have been reported to affect bacterial viability [38-42]. Here, we report on the results of a systematic study of the growth of *E.*

coli K12 on bare and biofunctionalized surfaces of bulk GaAs (001). We have compared these results with the growth of *E. coli* K12 on Au surfaces that have been known for their common use in biosensor research [16].

Experimental methods

Materials

Semi-insulating (SI) undoped GaAs (001) wafers (AXTG108-36) were obtained from AXT Inc. (Fremont, USA). OptiClear, acetone and isopropanol (2-propanol) used for cleaning the GaAs wafers were purchased from National Diagnostics (Mississauga, Canada), ACP Chemicals (Montréal, Canada) and Fisher Scientific (Ottawa, Canada), respectively. Anhydrous ethanol was obtained from Commercial Alcohols Inc. (Brampton, Canada). Deionized (DI) water with an electrical resistivity of 18 MΩ.cm was obtained with a Millipore purification custom system built by Culligan (Quebec, Canada). Ultra-high purity nitrogen 5.0 UHP (99.999%) used for deoxygenation of the anhydrous ethanol and high purity nitrogen 4.8 HP (99.998%) used for drying the GaAs wafers were both purchased from Praxair Canada Inc. (Mississauga, Canada). Ammonium hydroxide 28% (NH_4OH) was obtained from Anachemia (Richmond, Canada). Biotinylated polyethylene glycol (b-PEG) thiols were bought from Prochimia Surfaces (Gdansk, Poland). Ammonium sulfide 48% (AS), Luria Bertani (LB) broth, phosphate buffered saline (PBS) solution (10X, pH 7.4), 16-Mercaptohexadecanoic acid (MHDA) thiol, hexadecanethiol (HDT), 1-Ethyl-3-(3-dimethylaminopropyl)-carbodiimide (EDC) and N-hydroxysuccinimide (NHS) were all obtained from Sigma-Aldrich (Ontario, Canada). Non-conjugated polyclonal antibodies (Ab) and polyclonal

biotinylated antibodies (b-Ab) against *E. coli* were both bought from ViroStat, Inc (Portland, ME). Neutravidin (NA) was purchased from Molecular Probes (Invitrogen, Burlington, Canada). Live *E. coli* K12 bacteria were obtained from the Department of Biology of the Université de Sherbrooke (Quebec, Canada). The Au-coated samples were made by deposition of a thin layer of Au (40 -50 nm) on glass substrates in the cleanroom of the Interdisciplinary Institute for Technological Innovation (3IT), Université de Sherbrooke (Quebec, Canada).

Biofunctionalization of GaAs (001) and Au surfaces

Samples of 2 mm × 2 mm were cleaved from GaAs (001) wafers and cleaned in an ultrasonic bath with OptiClear, acetone and isopropanol sequentially for 5 min each. Following the cleaning steps, the GaAs samples were dried under a flow of compressed nitrogen and etched in a solution of NH_4OH (28%) for 2 min at room temperature. Three different bio-architectures have been applied to functionalize the surface of freshly etched GaAs (001) samples, as described below. The Au-coated glass samples, 2 mm × 2 mm, were cleaned in OptiClear, acetone and isopropanol, and then dried with a flow of compressed nitrogen. Dried samples were functionalized with MHDA-EDC/NHS-Ab in the same way as the GaAs samples.

b-PEG-NA-b-Ab functionalization

Freshly etched GaAs samples were rinsed with deoxygenated anhydrous ethanol and immediately incubated for 20 h at room temperature in a 2 mM mixture of b-PEG (1:15) and HDT (14:15) thiols diluted in deoxygenated anhydrous ethanol. After the thiolation

step, the GaAs samples were rinsed with deoxygenated anhydrous ethanol and exposed to AS (0.1%) for 15 min. Following this step, the samples were rinsed with DI water and incubated for 2 h at room temperature in PBS (1X) solution containing 200 µg/mL of neutravidin. Thereafter, the neutravidin-coated samples were immersed for 1 h at room temperature in a solution of biotinylated polyclonal antibodies against *E. coli* diluted in PBS (1X) at 0.1 mg/mL. The antibodies were biotinylated by the manufacturer by covalent attachment of biotin molecules to free amine groups (NH_2) in the antibody structure. Figure 1 shows a schematic illustration of bacteria immobilized on the GaAs (001) surface functionalized with an architecture comprising mixed b-PEG and HDT thiols, neutravidin and biotinylated polyclonal antibodies against *E. coli* (b-PEG-NA-b-Ab). The formation of HDT self-assembled monolayers (SAMs) on the GaAs (001) surface has been investigated with PL [43-46], ellipsometry [47], X-ray diffraction [48] and Fourier transform infrared spectroscopy (FTIR) [45]. The SAM formation from b-PEG diluted in OH-terminated PEG thiols has also been investigated using FTIR [49]. In each case, the intensity and full-width-at-half-maximum of two peaks in the 2800 to 3000 cm^{-1} region, that are assigned to stretching vibrations of CH_2 in the alkane chains [50], are considered as a measure of the quality of formed SAMs. Mixed SAMs comprising different thiols have also been investigated on Au surfaces [51-56], suggesting the feasibility of formation of such architectures on GaAs (001) surfaces as well. We employed the b-PEG-NA-b-Ab architecture to support the growth of bacteria on GaAs samples placed on nutrient LB-agar plates. A similar architecture was previously used by us for detection of *E. coli* K12 bacteria [26, 27].

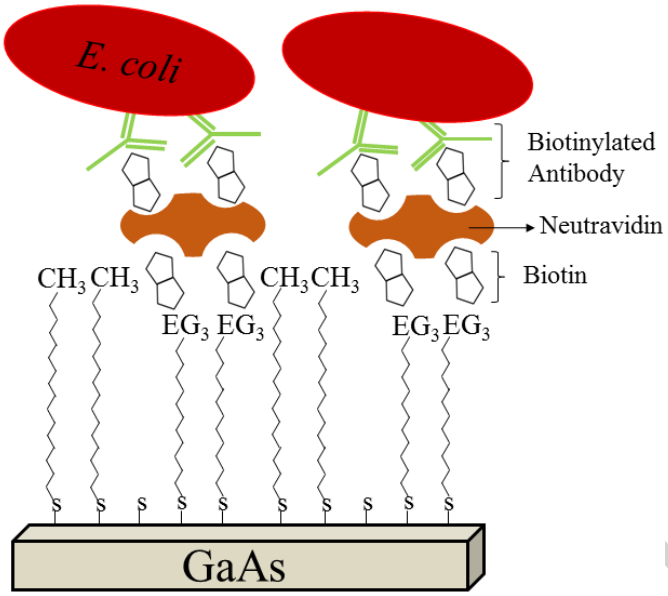

Fig. 1 Schematic illustration of a GaAs (001) surface functionalized with a biotinylated PEG-neutravidin-biotinylated antibody architecture for immobilization of *E. coli* bacteria.

MHDA-EDC/NHS functionalization

Freshly etched GaAs samples were rinsed with deoxygenated anhydrous ethanol and immediately incubated for 20 h at room temperature in a 2 mM solution of MHDA thiol diluted in deoxygenated anhydrous ethanol. Following this step, the GaAs samples were rinsed with deoxygenated anhydrous ethanol and then PBS (1X). Thereafter, the samples were incubated for 30 min at room temperature in a mixture of 400 mM of EDC and 100 mM of NHS diluted in PBS (1X) to activate the COOH group of the MHDA thiol. A schematic illustration of the MHDA-EDC/NHS biofunctionalization procedure applied to immobilize *E. coli* bacteria on the GaAs (001) surface is presented in Fig. 2. The formation of MHDA SAM on the GaAs (001) surface and activation of COOH group of this thiol with the EDC/NHS step has recently been discussed by Lacour et al. [57]. The

appearance of a C=O peak at 1741 cm^{-1} in FTIR absorption spectra of MHDA-coated samples that follows the EDC/NHS exposure, confirms the activation of the COOH group of MHDA thiol [58]. This process allows direct attachment of bacteria through covalent binding with naturally-occurring NH_2 groups on the bacterial surface [59]. The EDC/NHS activated MHDA SAM architecture has been applied to directly capture *E. coli* bacteria on GaAs samples kept in a flow cell.

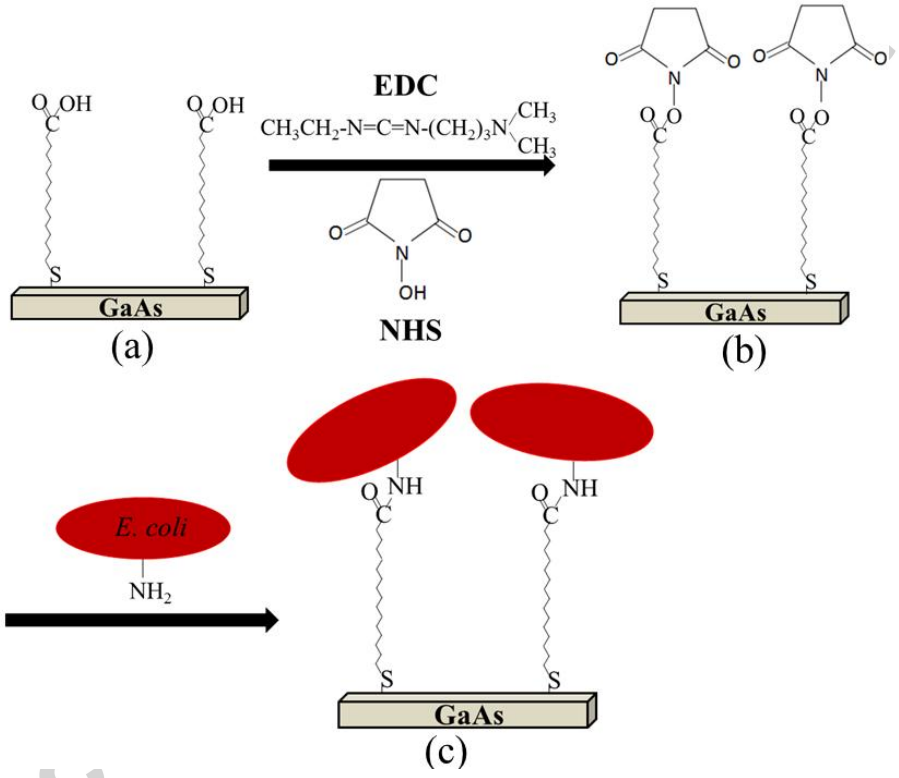

Fig. 2 Schematic illustration of the biofunctionalization steps employed for non-specific immobilization of *E. coli* bacteria on the surface of GaAs (001). Following formation of MHDA SAM on the freshly etched surface of GaAs (001) (a), COOH group of MHDA thiol is activated with EDC/NHS (b), which allows immobilization of *E. coli* via naturally-occurring NH_2 groups on the bacterial surface (c).

MHDA-EDC/NHS-Ab functionalization

The fabrication of MHDA-EDC/NHS-Ab bio-architecture on GaAs (001) and Au surfaces included covalent linkage of polyclonal Ab against *E. coli* to COOH groups of MHDA SAM that had been activated by EDC/NHS, as described in the previous section. The reaction was carried out for 1 h at room temperature from an antibody solution in PBS (1X) at 0.1 mg/mL. The illustration of the biofunctionalization steps employed in this case is presented schematically in Fig. 3. The immobilization of antibodies depended on covalent binding of their NH_2 groups with carboxyl-functionalized surfaces activated by EDC/NHS. As demonstrated by Lacour et al. with FTIR measurements [57], the presence of amide A, amide I and amide II bands in the 3300, 1660 and 1520 cm^{-1} regions [57, 60] validate the attachment of *E. coli* Ab to the GaAs (001) surface. This architecture has been applied to specifically capture *E. coli* bacteria on GaAs and Au samples kept in a flow cell. We note that no special procedure was employed to block activated COOH against reaction with bacteria (in MHDA-EDC/NHS bio-architecture) or with antibodies (in MHDA-EDC/NHS-Ab bio-architecture). It is reasonable, however, to expect that the LB growth medium contributed to the saturation of free COOH.

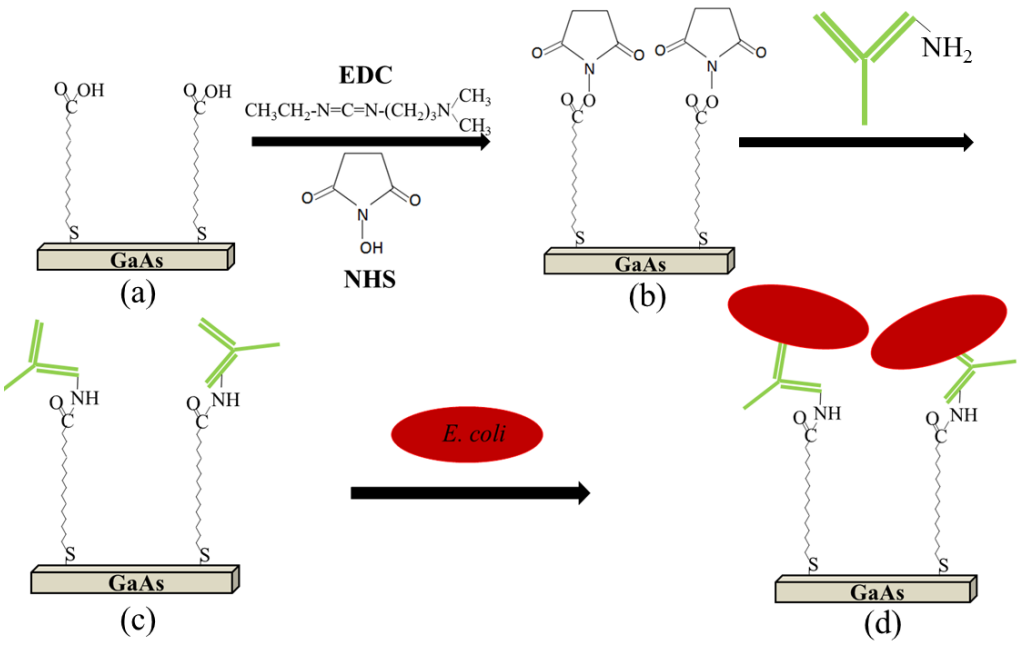

Fig. 3 Schematic illustration of the biofunctionalization steps applied for immobilization of *E. coli* bacteria with antibody on the surface of GaAs (001). Following formation of MHDA SAM on the freshly etched surface of GaAs (001) (a), COOH group of MHDA thiol is activated with EDC/NHS (b), followed by immobilization of *E. coli* antibodies whose NH_2 groups react with the EDC/NHS activated carboxyl sites (c), and antibody specific immobilization of *E. coli* bacteria (d).

Growth of *E. coli* on GaAs (001) and Au surfaces in contact with nutrient LB-agar plate

Freshly cultured *E. coli* K12 suspension was prepared by overnight growth of bacteria in LB at 37º C before use the following morning. The concentration of the bacteria was measured with a cell density meter (Fisher Scientific, model 40) operating at 600 nm. Bacteria were then centrifuged in LB for 25 min at 3000 rpm. After that, the medium was removed and the pellets were suspended in PBS (1X) and centrifuged at 3000 rpm for 15

min. Finally, PBS (1X) was removed and the pellets were resuspended in PBS (1X) and diluted to give 10^5 CFU/mL. A group of 8 b-PEG-NA-b-Ab functionalized and 8 bare GaAs (001) samples were placed upside down on a nutrient agar plate that had been inoculated evenly with 100 µL of the bacterial suspension at 10^5 CFU/mL in analogous fashion to a Kirby-Bauer disk diffusion antibiotic sensitivity test [61]. Assuming homogenous distribution of bacteria on the nutrient agar plate, the initial coverage of the agar plate with bacteria was around 2 bacteria/mm^2. This number was calculated by dividing the total number of bacteria used to inoculate the agar plate (10^4 bacteria) by the total area of the agar plate (45.6 cm^2). Figure 4 schematically illustrates the top and side views of the experimental setup. The plate with GaAs samples was then kept at 37° C for up to 8 hours.

Every hour, one of the bare samples and one of the biofunctionalized samples were removed from the agar plate and adherent bacteria were counted with an optical microscope following the procedure discussed in the Microscopic enumeration of bacteria section. These measurements allowed us to investigate the dynamics of the immobilization process on the surface of both samples. As a control experiment, a series of experiments was also carried out for bare Au samples following the methodology applied for GaAs (001) samples. The principle of studying the growth of bacteria on GaAs and Au samples in contact with bacterial cultures on Petri dishes can be compared to a Kirby–Bauer antibiotic sensitivity test [1, 9] where paper disks containing different types of antibiotics are placed on Petri dishes to allow evaluation of the impact of the antibiotics on bacterial growth.

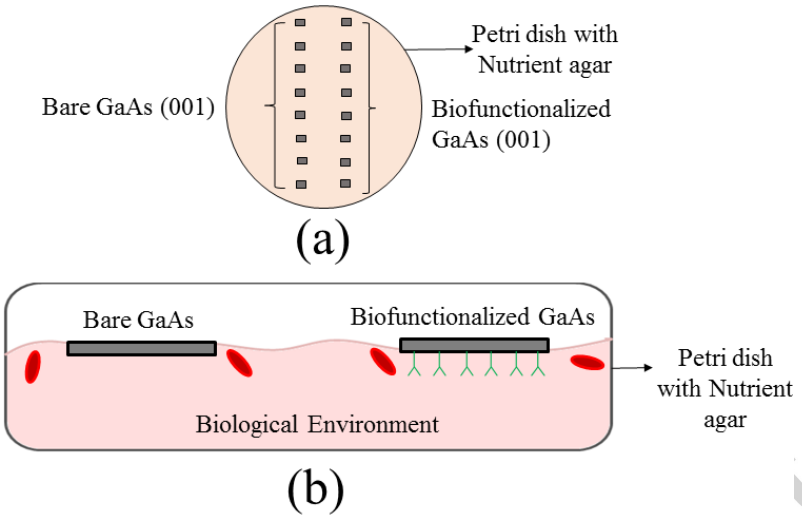

Fig. 4 Top view (a) and side view (b) of the setup for studying the growth of *E. coli* in proximity of GaAs samples. The nutrient agar plate was inoculated evenly with 100 µL of *E. coli* K12 bacteria (red ovals in (b)) at 10^5 CFU/mL. Biofunctionalized and bare GaAs (001) samples were placed upside down. The same setup and procedure was applied for bare Au samples.

Growth of *E. coli* on the surface of GaAs (001) and Au in a flow cell

In this approach, growth of *E. coli* K12 bacteria on biofunctionalized GaAs (001) and Au surfaces was investigated for samples kept in an ULTEM™ flow cell and exposed to bacterial suspensions and LB broth, sequentially. A schematic illustration of the setup used in this experiment is presented in Fig. 5. It consists of a flow cell with an outer diameter of 38.1 mm and a height of 3.92 mm. The flow cell contains a 150 µL groove for mounting samples and exposing them to bacterial solutions. Following the exposure, the samples were rinsed with LB medium stored in a dedicated vessel. The injection of fluids to the cell was achieved with a peristaltic pump and a 0.89 mm diameter

Santoprene tube. This setup is similar to that employed for monitoring PL *in situ* from GaAs/AlGaAs biochips exposed to different bacterial solutions [27, 28].

Following 10 min injection of 1 mL of freshly-cultured bacterial suspension into the flow cell (flow rate of 0.1 mL/min), the samples were left in contact with the bacterial suspension for an additional 20 min without any further injection. This resulted in a total of 30 min exposure of the samples to specific bacterial solutions, similar to that used by others for antigen-antibody reactions at liquid/solid interfaces [62]. Following this step, LB was injected into the flow cell for 30 min (flow rate of 0.1 mL/min) to replace 20 times the liquid volume of the flow cell groove, and to rinse away unattached bacteria. The bacteria were exposed to LB for an additional 4 h without any further injection while the flow cell was kept at 37° C to stimulate the growth of bacteria. The biochips were analyzed after 30 min exposure to bacterial suspension and after an additional 4.5 h exposure to LB broth with an optical microscope as described in the Section on Microscopic enumeration of bacteria. We performed this experiment for bacterial concentrations ranging from 10^4 to 10^8 CFU/mL and GaAs samples functionalized with MHDA-EDC/NHS and MHDA-EDC/NHS-Ab architectures. This allowed an investigation of the impact of different binding architectures on the initial capture and the subsequent growth of bacteria. The growth index of bacteria was also addressed as a function of the initial bacterial concentration for each bio-architecture. As a control, the same setup and procedure were applied for Au samples functionalized with MHDA-EDC/NHS-Ab and exposed to initial bacterial suspensions at 10^4 and 10^5 CFU/mL. Since the first step of our experiments was immobilization of bacteria on the surface of the

biochips, we only worked with biofunctionalized GaAs or Au samples and did not employ bare samples that are not able to efficiently capture the bacteria.

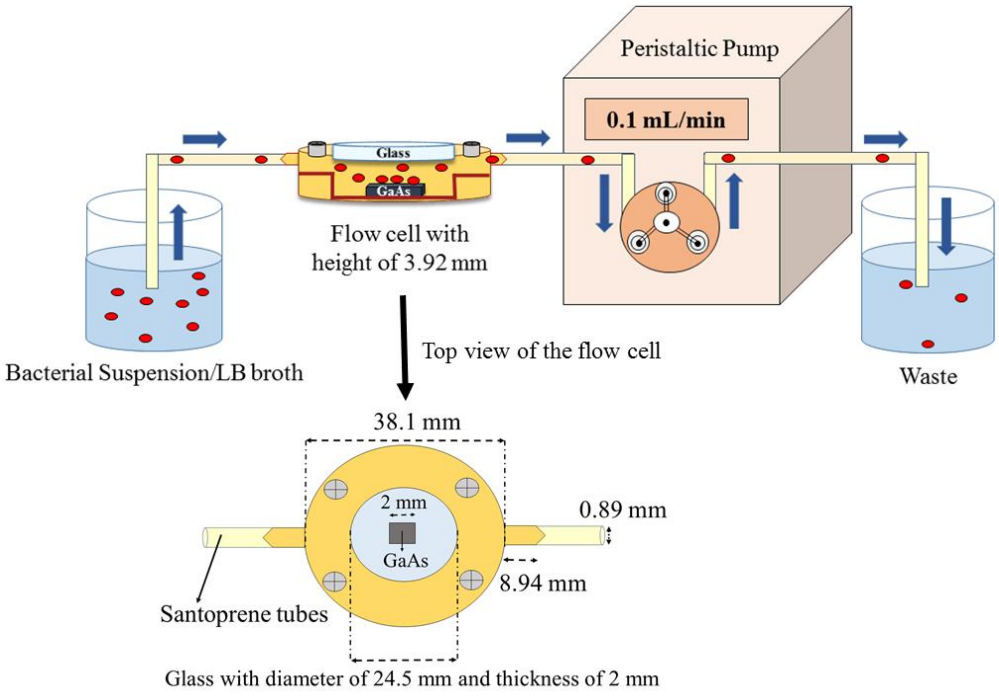

Fig. 5 Schematic illustration of the flow cell setup. The biofunctionalized GaAs (001) or Au biochips were placed in the flow cell and exposed to bacterial suspension (red ovals) and LB, sequentially. The bacteria and LB were injected into the flow cell at a flow rate of 0.1 mL/min using the peristaltic pump.

Microscopic enumeration of bacteria

Biochips were removed after each experiment and placed on glass slides, with the bacteria exposed surface facing up, for microscopic analysis. Without fixation, washing, or staining, bacteria were observed with an optical microscope (Zeiss, Axiotech) using overhead illumination. Bacteria were readily observed through a 100X lens and with a

supplemental 10X digital enlargement. Total concentration of bacteria adhered to the surface in each experiment was estimated by analyzing several optical images at magnification of 1000X (each image with the surface area of ~3500 μm^2 per field) collected at different sites of the sample and reported per mm^2.

Statistical methods

Similar sets of experiments, either for flow cell or Petri dish tests, were repeated at least 3 times to determine experimental error. This allowed us to calculate mean values of surface coverage with standard deviations.

Results and discussion

Growth of *E. coli* K12 on the surface of GaAs (001) and Au samples in contact with a nutrient agar plate

The growth of *E. coli* K12 was observed on both bare and b-PEG-NA-b-Ab functionalized surfaces of GaAs (001) biochips placed on nutrient agar plates. Not only was there no inhibition zone around the biochips as has been observed in similar experiments with silver nanoparticles [63], but neither bare nor functionalized GaAs samples prevented bacteria from multiplying. Figure 6 shows an optical image of an *E. coli* inoculated Petri dish with two GaAs chips (indicated by arrows) that remained in contact with the bacteria growth medium at 37 °C during a 24 h exposure. This experiment, inspired by the Kirby-Bauer disk diffusion antibiotic sensitivity test [61],

indicates that GaAs does not inhibit the growth of *E. coli* as it can be seen that bacteria grew abundantly next to the contact with the GaAs chips.

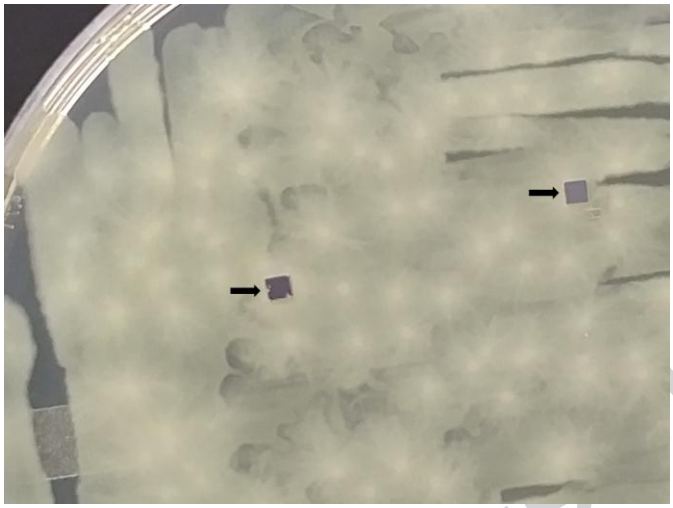

Fig. 6 Optical image of a Petri dish inoculated with *E. coli*. Two GaAs wafers (indicated with arrows) were placed on the surface. After 24 h of growth at 37°C, the Petri dish was photographed showing that bacteria grew abundantly next to the GaAs wafers.

The time dependent surface density of immobilized bacteria on bare and b-PEG-NA-b-Ab functionalized surfaces of GaAs (001) is illustrated in Fig. 7(a). The number of bacteria immobilized on the bare GaAs increased from 3±1 bacteria/mm^2 at 1 h to 2687±173 bacteria/mm^2 at 8 h. This compares with 20±3 and 2967±339 bacteria at 1 and 8 h for the biofunctionalized samples. The greater initial concentration of bacteria on the biofunctionalized surface suggests, as expected, more efficient capture of bacteria. The number of bacteria visualized on the GaAs surfaces probably reflected both non-specific and specific capture. It can be seen that initially (1 hour), the number of bacteria captured with Ab-based architectures exceeded ~ 7X the number of non-specifically captured

bacteria. However, after 6 hours, in both cases, the surface coverage with bacteria reached a saturation number of around 3×10^3 bacteria/mm^2. The saturation effect might be related to the stationary phase of bacterial growth when the rates of bacterial growth and bacterial death are equal [64, 65].

The data in Fig. 7(a), fitted with exponential curves, suggest that the number of bacteria doubled every 31 and 44 min on the surface of bare and antibody functionalized GaAs, respectively. This compares to the ability of *E. coli* to double every 20 min under ideal conditions of temperature, oxygen concentration and a rich liquid nutrient medium [66]. However, for comparable growth rates of bacteria in the exponential phase in liquid and solid environments (agar plates), the longer latency phase of bacteria on solid media could explain the lower rate of bacterial growth on solid substrates than in liquid environments [65]. This test demonstrates the feasibility of growing *E. coli* bacteria on GaAs (001) biochips placed on agar plates.

Figure 7(b) illustrates the time dependent surface density of *E. coli* bacteria immobilized on bare GaAs and Au samples. The number of bacteria immobilized on bare Au samples increased from 8±2 bacteria/mm^2 at 1 h to 2955±341 bacteria/mm^2 at 8 h. Fitted with the exponential curve, the number of bacteria in this case doubled every 35 min, which compares to the 31 min required by bacteria to double on the surface of bare GaAs. Thus, the similar growth rates of bacteria on bare GaAs and Au samples indicate that GaAs was no more inhibitory to the growth of *E. coli* bacteria than Au for the biochips placed on nutrient agar Petri dishes inoculated with bacteria.

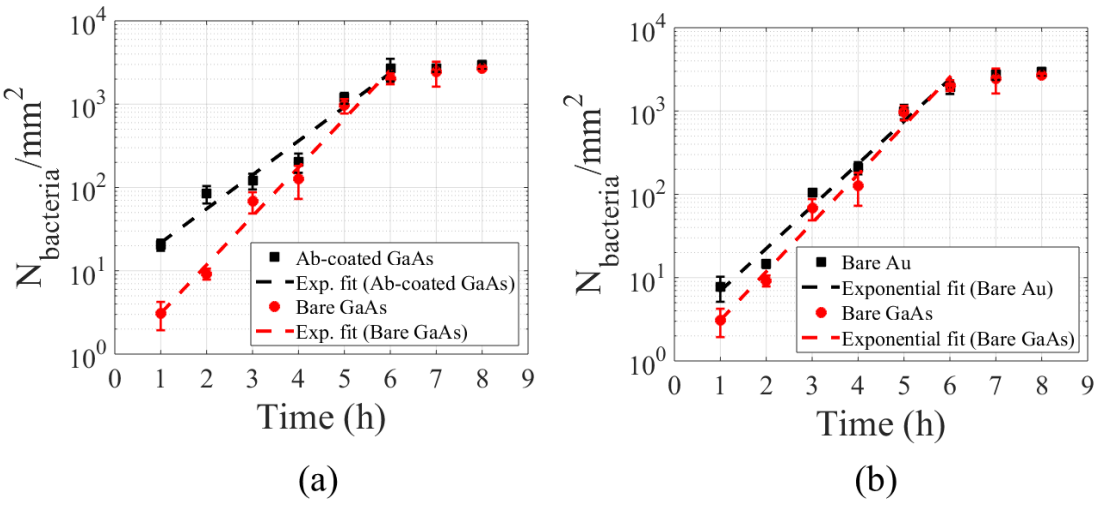

Fig. 7 Time dependent surface density of *E. coli* bacteria immobilized on bare and b-PEG-NA-b-Ab functionalized surfaces of GaAs (001) (a) and on bare Au surfaces compared to those of bare GaAs (b). Each experiment was repeated in triplicate to obtain the mean values with standard deviation.

Growth of *E. coli* K12 on GaAs (001) and Au surfaces in a flow cell

Figure 8 presents the initial surface coverage (after 30 min exposure to a bacterial suspension) and the coverage after a 4.5-h incubation in LB medium for GaAs biochips functionalized with MHDA-EDC/NHS and MHDA-EDC/NHS-Ab (See related data included in Supplementary Material). For the set of bacterial suspensions ranging from 10^5, 10^6, 10^7 and 10^8 CFU/mL, each experiment was performed at least in triplicate. Examples of optical images for a biochip functionalized with MHDA-EDC/NHS-Ab and exposed to bacterial suspension at 10^6 CFU/mL, before and after incubation in LB, are shown in Figure 9. We noted that the size of the bacteria before and after growth was in good agreement with literature data, indicating increased bacterial length after entering

the growth phase [67]. All bacteria appeared to be immobilized on the surface and not free in the film of LB medium that surrounded the sample because no bacteria could be seen moving by Brownian or flagella-assisted movement, nor were any partially out of the plane of focus as would be observed if the bacteria were free in the film of LB medium above the wafer surface. Theoretically, it would have been possible for bacteria to grow in the medium and then attach to the surface. This is very unlikely in this experiment as the flow cell was abundantly washed to remove unattached bacteria at the beginning of the experiment. If a few remaining bacteria had grown, subsequent attachment is quite inefficient. Indeed, when we add 10^6 bacteria to the flow cell, only 176±20 and 112±24 attach for MHDA-EDC/NHS-Ab and MHDA-EDC/NHS architectures respectively, so the majority of these bacteria would have still been floating in the LB medium and thus moving out of focus. For these reasons, we attributed increased coverage with surface growth rather than with growth free in the medium and subsequent attachment. The fact that no bacterial movement was observed during microscopic analysis cannot be explained by the bacteria being dead as even dead bacteria move extensively by Brownian movement. Since no heating was applied for fixation of bacteria to the surface, the bacterial immobility must be a result of attachment via antibodies.

The average growth index of bacteria was calculated for each bio-architecture and for each concentration of bacteria, and is presented in Table 1. The average growth index of bacteria was calculated using the following formula:

$$GI = \frac{N_2 / N_1}{T} \quad (1)$$

where N_1 and N_2 correspond to the surface coverage with bacteria before and after bacterial growth, respectively, and T is the duration of the experiment, which is equal to 300 min.

We systematically observed a greater initial surface coverage with *E. coli* using the EDC/NHS-Ab capture method compared with the direct EDC/NHS method for comparable concentrations of bacteria. The difference between the two bio-architectures in terms of the initial surface coverage was more noticeable for lower concentrations of bacteria. This might be related to a limitation in the number of bacteria that the antibody-coated surface is able to capture and saturation of this surface at higher bacterial concentrations. Due to the higher efficiency of antibody-coated surface in initial capture of bacteria, the surface coverage after bacterial growth (see Figure 8), and the bacterial growth index (see Table 1) were higher compared with the EDC/NHS functionalized surface for each concentration of bacteria. It is also possible that the lower number of bacteria on the EDC/NHS functionalized surface compared with antibody-coated surface, might be related to the reduced capture of growing bacteria directly on the EDC/NHS functionalized surface due to the inactivation of COO-NHS groups following their reaction with free NH_2 groups of proteins in the LB medium. In addition to the better conditions that antibody-coated surfaces offer for bacterial growth, they possess other advantages over EDC/NHS functionalized surfaces. In general, polyclonal antibodies, which were employed in MHDA-EDC/NHS-Ab bio-architecture, identify multiple epitopes on one antigenic macromolecule, therefore, they provide high affinity with bacteria. Besides that, application of GaAs samples functionalized with antibodies enables us to investigate growth of specific bacteria, while MHDA-EDC/NHS captures

bacteria non-specifically. We also investigated the capture efficiency of two antibody-coated architectures, MHDA-EDC/NHS-Ab and b-PEG-NA-b-Ab. We noticed that, for comparable concentrations of bacteria, the surface coverage with bacteria was higher on b-PEG-NA-b-Ab compared with MHDA-EDC/NHS-Ab. The reason might be related to the non-specific capture of bacteria with neutravidin used in b-PEG-NA-b-Ab. As an example, the initial coverage with bacteria, after 30 min exposure to bacterial suspension at 10^7 CFU/mL on b-PEG-NA-b-Ab was 410±112 bacteria/mm^2, while the coverage on MHDA-EDC/NHS-Ab was only 72±6 bacteria/mm^2.

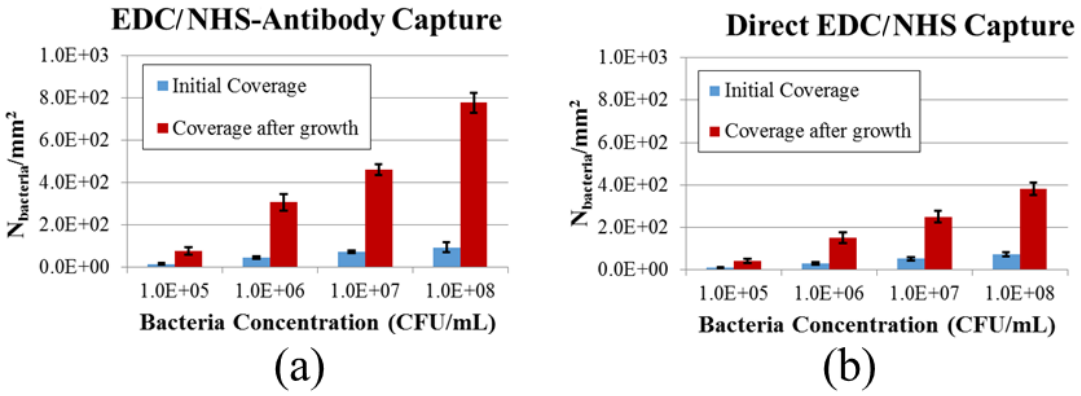

Fig. 8 Growth of *E. coli* on GaAs biochips functionalized with EDC/NHS-Ab (a), and EDC/NHS without antibody (b), detected by measuring initial (after 30 min exposure to a bacterial suspension) and final (after 4.5 h in LB) bacterial surface coverage for different concentrations of bacteria. Standard deviations were calculated based on experiments repeated in triplicate.

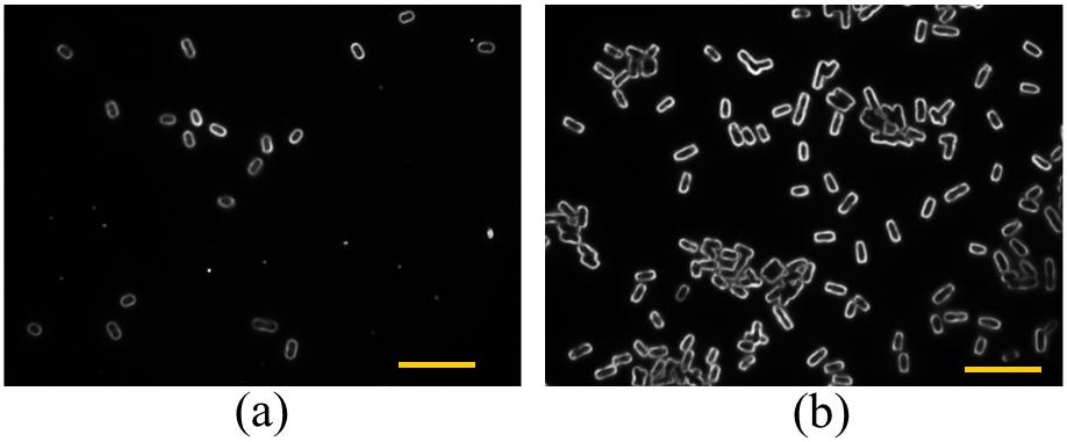

Fig. 9 Examples of microscopic images of *E. coli* K12 bacteria immobilized on the MHDA-EDC/NHS-Ab functionalized surface of GaAs (001) exposed for 30 min to a 10^6 CFU/mL solution (a), and after 4.5 h exposure to a growth medium (b). The scale bars correspond to 10 µm.

Table 1 Growth indices of bacteria on functionalized surfaces of GaAs (001) for different bacterial concentrations.

Bacterial concentration (CFU/mL)	**Growth index with EDC/NHS-Ab capture method (min^{-1})**	**Growth index with EDC/NHS capture method (min^{-1})**
10^5	0.0157± 0.0010	0.0148±0.0000
10^6	0.0231±0.0003	0.0180±0.0009
10^7	0.0213±0.0006	0.0160±0.0008
10^8	0.0287±0.0056	0.0180±0.0011

We were not able to observe the growth of bacteria on either of the investigated architectures for bacterial concentration of 10^4 CFU/mL. A minimum threshold concentration for bacterial growth might be related to the toxicity of Ga and As ions that

are known to affect the viability and/or growth of bacteria [38-42]. The release of these ions is a consequence of GaAs corrosion according to the following formula [68]:

$$GaAs + 2H_2O + 6h^+ \rightarrow Ga^{3+} + HAsO_2 + 3H^+ \quad (2)$$

It is possible that for bacterial concentrations below 10^5 CFU/mL, the amount of Ga and/or As ions released per bacteria could reach a toxic dose [39, 69] and, thus, affect bacterial viability and growth. Moreover, the growth of bacteria might also be inhibited by the antibodies used to capture bacteria in MHDA-EDC/NHS-Ab bio-architecture [70, 71].

As a control, we investigated the growth of *E. coli* on Au substrates functionalized with MHDA-EDC/NHS-Ab. Following the methodology applied for GaAs samples, the biofunctionalized Au samples were kept in the flow cell and exposed to the bacterial suspension at 10^5 CFU/mL and then to LB medium. The initial coverage of Au samples exposed for 30 min to the bacterial suspension and for 4.5 h to LB medium was at 17±5 and 98±25 bacteria/mm^2, respectively. The average bacterial growth index of 0.019 min^{-1} on these samples was slightly higher than that of 0.016 min^{-1} on MHDA-EDC/NHS-Ab functionalized GaAs samples, suggesting that for the 10^5 CFU/mL solution, the GaAs substrate had only a minor negative effect on bacterial growth in comparison to the Au substrate. We note that the Petri dish experiments with GaAs (001) and Au substrates in contact with nutrient agar plates inoculated with bacteria at ~ 2 bacteria/mm^2, revealed comparable growth rates of bacteria on both bare GaAs and Au substrates. This suggests that the concentration of As and/or Ga released to the Petri dish was not sufficient to affect bacterial growth, or that the agar growth medium neutralized any toxicity. Given

that some toxicity has been observed for Au in an ionic form [37], our inability to observe bacterial growth on both Au and GaAs substrates kept in the flow cell, when initial concentrations of bacteria were below 10^5 CFU/mL, could be due to comparable toxicity of the Au and GaAs substrates. Nevertheless, these results have revealed that the GaAs surface provides conditions satisfactory for the growth of bacteria in a flow cell, which potentially is attractive for photonic monitoring *in situ* of the growth and reaction of bacteria to different biological environments and particularly antibiotics.

Conclusion

In our endeavour to develop a GaAs-based photonic biosensor for monitoring reaction of bacteria to different biochemical conditions, we have investigated the capture and growth of *E. coli* K12 on surfaces of GaAs (001). The experiments with bare GaAs and Au in contact with nutrient agar plates inoculated with bacteria at ~ 2 bacteria/mm^2 suggested that neither of these substrates inhibited the growth of bacteria. However, the experiments in a flow cell revealed that the initial coverage, and the subsequent bacterial growth were dependent on the biofunctionalization architecture used to capture bacteria. Antibody biofunctionalized surfaces exhibited significantly higher capture efficiencies, especially at lower concentrations of bacteria. For suspensions containing bacteria at less than 10^5 CFU/mL, we were not able to observe the growth of bacteria, regardless of the biofunctionalization architecture. This threshold might be related to the toxicity of As and/or Ga released from the GaAs samples. While different methods could be investigated to address this issue and reduce the potential effect of toxicity of As and/of Ga ions, we note that a similar shortcoming characterizes matrix-assisted laser desorption

ionization time of flight mass spectrometry (MALDI-TOF MS) which requires 10^4 – 10^5 cells per assay [72], yet is about to revolutionize clinical diagnostic laboratories. Whereas MALDI-TOF MS does not determine antibiotic sensitivity, our approach does [33] and could thus complement MALDI-TOF MS in the same time frame. However, it is expected that by increasing the initial surface coverage with bacteria we could observe bacterial growth at concentrations lower than 10^5 CFU/mL. The reason is that by increasing the number of bacteria immobilized on the surface, the ratio of Ga and/or As per bacteria decreases and, consequently, the dose might not reach the toxic levels. Increasing the surface coverage with bacteria could be achieved by improving surface functionalization techniques, or by applying some methods such as chemotaxis [73], filtration [74] or electrophoresis [75].

Funding

This work was supported by the Canada Research Chair in Quantum Semiconductors Program (Grant No 950-220304) and the Fonds de recherche Nature et Technologie du Québec (FRQNT) project (Grant number 2015-PR-184056).

Acknowledgements

We thank Dr. Khalid Moumanis and the technical staff of the Interdisciplinary Institute for Technological Innovation (3IT) for their assistance. We are also indebted to Dr. François Malouin of the Department of Biology, Université de Sherbrooke for kindly supplying *E. coli* K12.

References

[1] J. Versalovic, K.C. Carroll, G. Funke, J.H. Jorgensen, M.L. Landry, D.W. Warnock, Manual of Clinical Microbiology, tenth ed., American Society for Microbiology Press, Washington, 2011.
[2] B. Sonnleitner, G. Locher, A. Fiechter, Biomass determination, J. Biotechnol. 25 (1992) 5-22.
[3] M. Nayak, A. Kotian, S. Marathe, D. Chakravortty, Detection of microorganisms using biosensors—A smarter way towards detection techniques, Biosens. Bioelectron. 25(4) (2009) 661-667.
[4] J.E. Garneau, S. Moineau, Bacteriophages of lactic acid bacteria and their impact on milk fermentations, Microb. Cell Fact. 10(Suppl 1) (2011) S20-S20.
[5] M.M. Schuler, I.W. Marison, Real-time monitoring and control of microbial bioprocesses with focus on the specific growth rate: current state and perspectives, Appl. Microbiol. Biotechnol. 94(6) (2012) 1469-82.
[6] J.S. Kee, S.Y. Lim, A.P. Perera, Y. Zhang, M.K. Park, Plasmonic nanohole arrays for monitoring growth of bacteria and antibiotic susceptibility test, Sens. Actuator B-Chem. 182 (2013) 576–583.
[7] V. de Freitas, E. Carvalho, N. Mateus, Study of carbohydrate influence on protein-tannin aggregation by nephelometry, Food Chem. 81(4) (2003) 503-509.
[8] A. Joubert, B. Calmes, R. Berruyer, M. Pihet, J.P. Bouchara, P. Simoneau, T. Guillemette, Laser nephelometry applied in an automated microplate system to study filamentous fungus growth, Biotechniques 48(5) (2010) 399-404.
[9] J.A. Poupard, L.R. Walsh, B. Kleger, Antimicrobial Susceptibility Testing, Springer, New York, 1994.
[10] Y.L. Chiang, C.H. Lin, M.Y. Yen, Y.D. Su, S.J. Chen, H.F. Chen, Innovative antimicrobial susceptibility testing method using surface plasmon resonance, Biosens. Bioelectron. 24(7) (2009) 1905-10.
[11] J.M. Rolain, M.N. Mallet, P.E. Fournier, D. Raoult, Real-time PCR for universal antibiotic susceptibility testing, J. Antimicrob. Chemother. 54 (2004) 538–541.
[12] A. Cotto, J.K. Looper, L.C. Mota, A. Son, Quantitative polymerase chain reaction for microbial growth kinetics of mixed culture system, J. Microbiol. Biotechnol. 25(11) (2015) 1928-35.
[13] B.L. Roth, M. Poot, S.T. Yue, P.J. Millard, Bacterial viability and antibiotic susceptibility testing with SYTOX green nucleic acid stain, Appl. Environ. Microbiol. 63 (1997) 2421–2431.
[14] P. Boi, A. Manti, A. Pianetti, L. Sabatini, D. Sisti, M.B. Rocchi, F. Bruscolini, L. Galluzzi, S. Papa, Evaluation of *Escherichia coli* viability by flow cytometry: A method for determining bacterial responses to antibiotic exposure, Cytometry B. Clin. Cytom. 88(3) (2015) 149-53.
[15] S. Mwaigwisya, R.A. Assiri, J. O'Grady, Emerging commercial molecular tests for the diagnosis of bloodstream infection, Expert Rev. Mol. Diagn. 15(5) (2015) 681-92.
[16] O. Lazcka, F.J. Del Campo, F.X. Munoz, Pathogen detection: A perspective of traditional methods and biosensors, Biosens. Bioelectron. 22 (2007) 1205-1217.
[17] B. Adamowicz, K. Ikeya, M. Mutoh, T. Saitoh, H. Fujikura, H. Hasegawa, Photoluminescence characterization of air exposed AlGaAs surface and passivated ex situ by ultrathin silicon interface control layer, Physica E 2 (1998) 261-266.
[18] T.H. Gfroerer, Photoluminescence in Analysis of Surfaces and Interfaces, in: R.A. Meyers (Ed.), Encyclopedia of analytical chemistry : applications, theory and instrumentation, John Wiley & Sons, Ltd, Chichester, 2006, pp. 9209–9231.

[19] M.V. Lebedev, Role of sulfide ion solvation in the modification of GaAs surface electronic structure, Semiconductors+ 35(11) (2001) 1291-1299.
[20] K. Moumanis, X. Ding, J.J. Dubowski, E.H. Frost, Aging and detergent washing effects of the surface of (001) and (110) GaAs passivated with hexadecanethiol, J. Appl. Phys. 100(3) (2006) 034702.
[21] P. Tomkiewicz, S. Arabasz, B. Adamowicz, M. Miczek, J. Mizsei, D.R.T. Zahn, H. Hasegawa, J. Szuber, Surface electronic properties of sulfur-treated GaAs determined by surface photovoltage measurement and its computer simulation, Surf Sci 603(3) (2009) 498-502.
[22] F. Seker, K. Meeker, T.F. Kuech, A.B. Ellis, Surface chemistry of prototypical bulk II-VI and III-V semiconductors and implications for chemical sensing, Chem. Rev. 100 (2000) 2505-2536.
[23] Z. Zhang, J.T. Yates, Band bending in semiconductors: chemical and physical consequences at surfaces and interfaces, Chem. Rev. 112(10) (2012) 5520-5551.
[24] H.A. Budz, M.M. Ali, Y. Li, R.R. LaPierre, Photoluminescence model for a hybrid aptamer-GaAs optical biosensor, J. Appl. Phys. 107(10) (2010) 104702.
[25] J.J. Dubowski, X. Ding, E.H. Frost, E. Escher, Quantum dot template for fast and simultaneous detection of different infectious agents, United States Patent, NO. 11/908,223, 2014.
[26] V. Duplan, E.H. Frost, J.J. Dubowski, A photoluminescence-based quantum semiconductor biosensor for rapid in situ detection of *Escherichia coli*, Sens. Actuators B-Chem. 160 (2011) 46-51.
[27] E. Nazemi, S. Aithal, W.M. Hassen, E.H. Frost, J.J. Dubowski, GaAs/AlGaAs heterostructure photonic biosensor for rapid detection of *Escherichia coli* in phosphate buffered saline solution, Sens. Actuators B-Chem. 207 (2015) 556–562.
[28] M.R. Aziziyan, W.M. Hassen, D. Morris, E.H. Frost, J.J. Dubowski, Photonic biosensor based on photocorrosion of GaAs/AlGaAs quantum heterostructures for detection of Legionella pneumophila, Biointerphases 11(1) (2016) 019301.
[29] A. Ohtake, Surface reconstructions on GaAs(001), Surf. Sci. Rep. 63(7) (2008) 295-327.
[30] V.P. LaBella, M.R. Krause, Z. Ding, P.M. Thibado, Arsenic-rich GaAs(001) surface structure, Surf. Sci. Rep. 60 (2005) 1-53.
[31] O. Wada, Optoelectronic integration based on GaAs material, Opt. Quant. Electron. 20 (1988) 441-474.
[32] S. Mokkapati, C. Jagadish, III-V compound SC for optoelectronic devices, Mater. Today 12 (2009) 22-32.
[33] E. Nazemi, W.M. Hassen, E.H. Frost, J.J. Dubowski, Monitoring growth and antibiotic susceptibility of Escherichia coli with photoluminescence of GaAs/AlGaAs quantum well microstructures, Biosens Bioelectron 93 (2017) 234-240.
[34] V.N. Golubovich, I.L. Rabotnova, Kinetics of growth inhibition by silver ions, Microbiology 43 (1974) 948-950.
[35] A.L. Casey, T.J. Karpanen, P. Nightingale, M. Cook, T.S.J. Elliott, Microbiological comparison of a silver-coated and a non-coated needleless intravascular connector in clinical use, J. Hosp. Infect. 80(4) (2012) 299-303.
[36] Y. Zhou, Y. Kong, S. Kundu, J.D. Cirillo, H. Liang, Antibacterial activities of gold and silver nanoparticles against Escherichia coli and bacillus Calmette-Guerin, J. Nanobiotechnology 10 (2012) 19.
[37] D.N. Williams, S.H. Ehrman, T.R. Pulliam Holoman, Evaluation of the microbial growth response to inorganic nanoparticles, J. Nanobiotechnology 4(1) (2006) 1-8.
[38] P.I. Harvey, F.K. Crundwell, The effect of As(III) on the growth of *Thiobacillus ferrooxidans* in an electrolytic cell under controlled redox Potentials, Miner. Eng. 9(10) (1996) 1059-1068.

[39] V.I. Podol'skaia, T.G. Gruzina, Z.P. Ul'berg, A.S. Sokolovskaia, N.I. Grishchenko, Effect of arsenic on bacterial growth and plasma membrane atpase activity, Prikladnaia biokhimiia i mikrobiologiia 38(1) (2002) 57-62.
[40] O. Rzhepishevska, B. Ekstrand-Hammarstrom, M. Popp, E. Bjorn, A. Bucht, A. Sjostedt, H. Antti, M. Ramstedt, The antibacterial activity of Ga^{3+} is influenced by ligand complexation as well as the bacterial carbon source, Antimicrob. Agents Chemother. 55(12) (2011) 5568-80.
[41] K. DeLeon, F. Balldin, C. Watters, A. Hamood, J. Griswold, S. Sreedharan, K.P. Rumbaugh, Gallium maltolate treatment eradicates *Pseudomonas aeruginosa* infection in thermally injured mice, Antimicrob. Agents Chemother. 53(4) (2009) 1331-7.
[42] R. Mukhopadhyay, B.P. Rosen, L.T. Phung, S. Silver, Microbial arsenic: from geocycles to genes and enzymes, FEMS Microbiol. Rev. 26(3) (2002) 311-25.
[43] X.M. Ding, K. Moumanis, J.J. Dubowski, L. Tay, N.L. Rowell, Fourier-transform infrared and photoluminescence spectroscopies of self-assembled monolayers of long-chain thiols on (001) GaAs, J Appl Phys 99(5) (2006) 054701.
[44] C.K. Kim, G.M. Marshall, M. Martin, M. Bisson-Viens, Z. Wasilewski, J.J. Dubowski, Formation dynamics of hexadecanethiol self-assembled monolayers on (001) GaAs observed with photoluminescence and Fourier transform infrared spectroscopies, J Appl Phys 106(8) (2009) 083518.
[45] P. Arudra, G.M. Marshall, N. Liu, J.J. Dubowski, Enhanced Photonic Stability of GaAs in Aqueous Electrolyte Using Alkanethiol Self-Assembled Monolayers and Postprocessing with Ammonium Sulfide, J Phys Chem C 116 (2012) 2891-2895.
[46] X.H. Huang, J.J. Dubowski, Solvent-mediated self-assembly of hexadecanethiol on GaAs (001), Appl Surf Sci 299 (2014) 66-72.
[47] D.M. Rosu, J.C. Jones, J.W.P. Hsu, K.L. Kavanagh, D. Tsankov, U. Schade, N. Esser, K. Hinrichs, Molecular Orientation in Octanedithiol and Hexadecanethiol Monolayers on GaAs and Au Measured by Infrared Spectroscopic Ellipsometry, Langmuir 25(2) (2009) 919-923.
[48] C.L. McGuiness, D. Blasini, J.P. Masejewski, S. Uppili, O.M. Cabarcos, D. Smilgies, D.L. Allara, Molecular self-assembly at bare semiconductor surfaces: Characterization of a homologous series of n-alkanethiolate monolayers on GaAs(001), Acs Nano 1(1) (2007) 30-49.
[49] V. Duplan, Y. Miron, E.H. Frost, M. Grandbois, J.J. Dubowski, Specific immobilization of influenza A virus on GaAs (001) surface, J. Biomed. Opt. 14(5) (2009) 054042.
[50] R. Arnold, W. Azzam, A. Terfort, C. Wöll, Preparation, modification, and crystallinity of aliphatic and aromatic carboxylic acid terminated self-assembled monolayers, Langmuir 18(10) (2002) 3980–3992.
[51] J.P. Folkers, P.E. Laibinis, G.M. Whitesides, Self-assembled monolayers of alkanethiols on gold: Comparisons of monolayers containing mixtures of short-and long-chain constituents with CH_3 and CH_2OH terminal groups, Langmuir 8 (1992) 1330-1341.
[52] D.J. Olbris, A. Ulman, Y. Shnidman, Interplay of wetting and adsorption at mixed self-assembled monolayers, J. Chem. Phys. 102 (1995) 6865-6873.
[53] K.E. Nelson, L. Gamble, L.S. Jung, M.S. Boeckl, E. Naeemi, S.L. Golledge, T. Sasaki, D.G. Castner, C.T. Campbell, P.S. Stayton, Surface characterization of mixed self-assembled monolayers designed for streptavidin immobilization, Langmuir 17(9) (2001) 2807-2816.
[54] K. Yoshioka, Y. Sato, T. Murakami, M. Tanaka, O. Niwa, One-step detection of galectins on hybrid monolayer surface with protruding lactoside, Anal. Chem. 82(4) (2010) 1175-1178.
[55] R. Tarnawski, M. Ulbricht, Amphiphilic gold nanoparticles: Synthesis, characterization and adsorption to PEGylated polymer surfaces, Colloids Surf., A 374(1–3) (2011) 13-21.

[56] D.E. Mustafa, H. Fan, X. Zhou, H.Y. Tu, A.D. Zhang, Adsorption behaviour of PEGylated gold nanoparticles to different surfaces probed by CV monitoring, Adv. Mat. Res. 455-456 (2012) 689-695.
[57] V. Lacour, C. Elie-Caille, T. Leblois, J.J. Dubowski, Regeneration of a thiolated and antibody functionalized GaAs (001) surface using wet chemical processes, Biointerphases 11(1) (2016) 019302.
[58] B.L. Frey, R.M. Corn, Covalent attachment and derivatization of poly(l-lysine) monolayers on gold surfaces as characterized by polarization−modulation FT-IR spectroscopy, Anal. Chem. 68(18) (1996) 3187-3193.
[59] R.L. Meyer, X. Zhou, L. Tang, A. Arpanaei, P. Kingshott, F. Besenbacher, Immobilisation of living bacteria for AFM imaging under physiologicalconditions, Ultramicroscopy 110(11) (2010) 1349-57.
[60] J. Bandekar, Amid modes and protien conformation, Biochim. Biophys. Acta 1120 (1992) 123-143.
[61] A.W. Bauer, W.M. Kirby, J.C. Sherris, M. Turck, Antibiotic susceptibility testing by a standardized single disk method, Am. J. Clin. Pathol. 45(4) (1966) 493-6.
[62] V. Hlady, J.N. Lin, J.D. Andrade, Spatially resolved detection of antibody–antigen reaction on solid/liquid interface using total internal reflection excited antigen fluorescence and charge-coupled device detection, Biosens. Bioelectron. 5 (1990) 291–301.
[63] S.Z. Naqvi, U. Kiran, M.I. Ali, A. Jamal, A. Hameed, S. Ahmed, N. Ali, Combined efficacy of biologically synthesized silver nanoparticles and different antibiotics against multidrug-resistant bacteria, Int. J. Nanomedicine 8 (2013) 3187-95.
[64] T. Akerlund, K. Nordstorm, R. Bernander, Analysis of cell size and DNA content in exponentially growing and stationary phase batch cultures of *Escherichia coli*, J. Bacteriol. 177 (1995) 6791-6797.
[65] H. Fujikawa, S. Morozumi, Modeling surface growth of *Escherichia coli* on agar plates, Appl. Environ. Microbiol. 71(12) (2005) 7920-7926.
[66] H.C. Berg, *E. coli* in Motion, Springer, New York, 2004.
[67] F.J. Trueba, C.L. Woldringh, Changes in cell diameter during the division cycle of *Escherichia coli*, J. Bacteriol. 142 (1980) 869–878.
[68] M.N. Ruberto, X. Zhang, R. Scarmozzino, A.E. Willner, D.V. Podlesnik, R.M. Osgood Jr., The laser controlled micrometer scale photoelectrochemical etching of III–V semiconductors, J. Electrochem. Soc. 138 (1991) 1174-85.
[69] C. Diorio, J. Cai, J. Marmor, R. Shinder, M.S. DuBow, An *Escherichia coli* chromosomal ars operon homolog is functional in arsenic detoxification and is conserved in gram-negative bacteria, J. Bacteriol. 177(8) (1995) 2050-6.
[70] J. Lin, J.S. Hogan, K.L. Smith, Inhibition of in vitro growth of coliform bacteria by a monoclonal antibody directed against ferric enterobactin receptor FepA1, J. Dairy Sci. 81(5) (1998) 1267-1274.
[71] R. Chalghoumi, A. Thewis, Y. Beckers, C. Marcq, D. Portetelle, Y.J. Schneider, Adhesion and growth inhibitory effect of chicken egg yolk antibody (IgY) on Salmonella enterica serovars Enteritidis and Typhimurium in vitro, Foodborne Pathog. Dis. 6(5) (2009) 593-604.
[72] A. van Belkum, G. Durand, M. Peyret, S. Chatellier, G. Zambardi, J. Schrenzel, D. Shortridge, A. Engelhardt, W.M. Dunne, Jr., Rapid clinical bacteriology and its future impact, Ann Lab Med 33(1) (2013) 14-27.
[73] W.M. Hassen, H. Sanyal, M. Hammood, K. Moumanis, E.H. Frost, J.J. Dubowski, Chemotaxis for enhanced immobilization of Escherichia coli and Legionella pneumophila on biofunctionalized surfaces of GaAs, Biointerphases 11(2) (2016) 021004.

[74] X. Wu, C. Han, J. Chen, Y.-W. Huang, Y. Zhao, Rapid Detection of Pathogenic Bacteria from Fresh Produce by Filtration and Surface-Enhanced Raman Spectroscopy, JOM 68(4) (2016) 1156-1162.
[75] A. Bossi, S.A. Piletsky, P.G. Righetti, A.P.F. Turner, Capillary electrophoresis coupled to biosensor detection, Journal of Chromatography A 892(1–2) (2000) 143-153.

Research highlights

- Growth of *E. coli* in a Petri dish is not affected by the presence of a GaAs plate
- Antibody-functionalized GaAs provides attractive conditions for growth of bacteria
- Minimum concentration of bacteria at 10^5 CFU/mL is required to grow in a flow cell
- Important insight is provided to bioengineering of GaAs for biosensing applications